PROCEEDINGS OF SPIE

SPIEDigitalLibrary.org/conference-proceedings-of-spie

High-speed RZ-DPSK photonic integrated transmitter for space optical communications

Joseph Fridlander, Victoria Rosborough, Fengqiao Sang, Sergio Pinna, Steven Estrella, et al.

Joseph Fridlander, Victoria Rosborough, Fengqiao Sang, Sergio Pinna, Steven Estrella, Leif Johansson, Jonathan Klamkin, "High-speed RZ-DPSK photonic integrated transmitter for space optical communications," Proc. SPIE 11133, Laser Communication and Propagation through the Atmosphere and Oceans VIII, 1113309 (6 September 2019); doi: 10.1117/12.2528213

SPIE.

Event: SPIE Optical Engineering + Applications, 2019, San Diego, California, United States

High-Speed RZ-DPSK Photonic Integrated Transmitter for Space Optical Communications

Joseph Fridlander[a], Victoria Rosborough[a], Fengqiao Sang[a], Sergio Pinna[a], Steven Estrella[a,b], Leif Johansson[b], Jonathan Klamkin[a]
[a]Electrical and Computer Engineering, University of California, Santa Barbara, CA 93106, USA;
[b]Freedom Photonics, 41 Aero Camino, Santa Barbara, CA 93117, USA;

ABSTRACT

We report on a monolithic indium phosphide photonic integrated transmitter capable of generating high-speed return-to-zero differential phase shift keying (RZ-DPSK) data streams for space optical communications as high as 5 Gbps. The integrated transmitter includes a sampled grating distributed Bragg reflector laser continuously tunable over 30 nm in the C-band, a semiconductor optical amplifier for amplification, a Mach-Zehnder modulator for encoding phase-shift-keying data, and electro-absorption modulator for return-to-zero pulse carving. The transmitter is situated in a custom electronics test bed for biasing various PIC sections and driving the modulators. Furthermore, this transmitter can also be utilized for 10 Gbps DPSK or NRZ-OOK.

Keywords: Photonics integrated circuits, Free-space optical communications, Differential phase shift keying

1. INTRODUCTION

Space optical communication will help meet the bandwidth demands required for future earth science and space exploration missions. While RF transmitters require increasing complexity for communication over regulated narrow channel bandwidths, optical communication offers higher directivity and large swaths of bandwidth at optical wavelengths. These benefits were illustrated in recent years by several space agencies worldwide. In 2013 NASA's Lunar Laser Communications Demonstration (LLCD) established a high-speed link from an optical terminal in lunar orbit with a ground station. LLCD up-link and down-link data rates of 20 and 622 Mbps were demonstrated, respectively [1]. Low earth orbit satellites NFIRE and TerraSAR-X verified a 5.6 Gbps intersatellite optical link [2]. NASA plans to follow up LLCD with the Laser Communication Relay Demonstration (LCRD). Using optical terminals in geosynchronous orbit, LCRD will relay bi-directional data between optical ground stations at 1.244 Gbps [3].

Presently, optical communication terminals are constructed using discretely package optical devices. Photonics integrated circuits (PICs) on the other hand allow reduced cost, size, weight, and power (C-SWaP) by allowing integration of active functions such as lasers and modulators and passive functions such as filters, couplers, and power splitters on-chip. Furthermore, built-in test functions can be integrated beside the transmitter to ensure it is operating optimally. In addition to communication, by engineering the photonics integration platform and device geometries, photonics engineers can tailor PICs for use as primary science instruments. PIC applications range from optical transceivers, mm-wave, spectroscopy, lidar, and metrology to name a few [4-5]. For these same reasons PICs are a very attractive technology for small satellite platforms such as CuberSats which allow demonstration of new technology for space science and exploration at lower costs.

Previous promising work has shown PICs capable of 12.5 Mbps pulse position modulation [6] and 3 Gbps NRZ-OOK [7]. The PIC in this work is monolithically integrated on an InP integration platform, the most mature photonics platform. We demonstrate 5 Gbps RZ-DPSK modulation and 10 Gbps DPSK and NRZ-OOK. Relaxed linewidth requirements and non-coherent demodulation using only a delay line interferometer make DPSK an attractive modulation format for optical communication [8-9]. Furthermore, use of an average power limited amplifier in burst mode effectively allows multi rate communication. Compared to standard DPSK, RZ-DPSK improves the sensitivity of optically preamplified receivers [10].

Laser Communication and Propagation through the Atmosphere and Oceans VIII, edited by Jeremy P. Bos, Alexander M. J. van Eijk and Stephen Hammel, Proc. of SPIE Vol. 11133, 1113309
 · doi: 10.1117/12.2528213

2. TRANSMITTER OVERVIEW

Figure 1 shows the monolithically integrated transmitter PIC beside the driving electronics. The PIC consists of a sampled grating distributed Bragg reflector (SG-DBR) laser tunable over 30 nm in the telecommunications C-band. The SG-DBR, which is a four-section laser, allows continuous and wide tuning by current injection into the front and back mirrors and a phase section. Careful conditioning of the currents allows alignment of tunable mirror reflectivity peaks with a tunable longitudinal mode of the laser. A few selected wavelengths over the tuning range can be seen in figure 2. The SG-DBR also showed side mode suppression ratios exceeding 45 dB. Figure 3 shows a light-current-voltage plot of the laser on PIC. The threshold current is approximately 30 mA and the slope efficiency is 0.1 W/A. The output power from the laser, which was measured by reverse biasing a semiconductor optical amplifier (SOA) following the laser and assuming a 1A/W responsivity, exceeded 7 mW at a current drive of 100 mA.

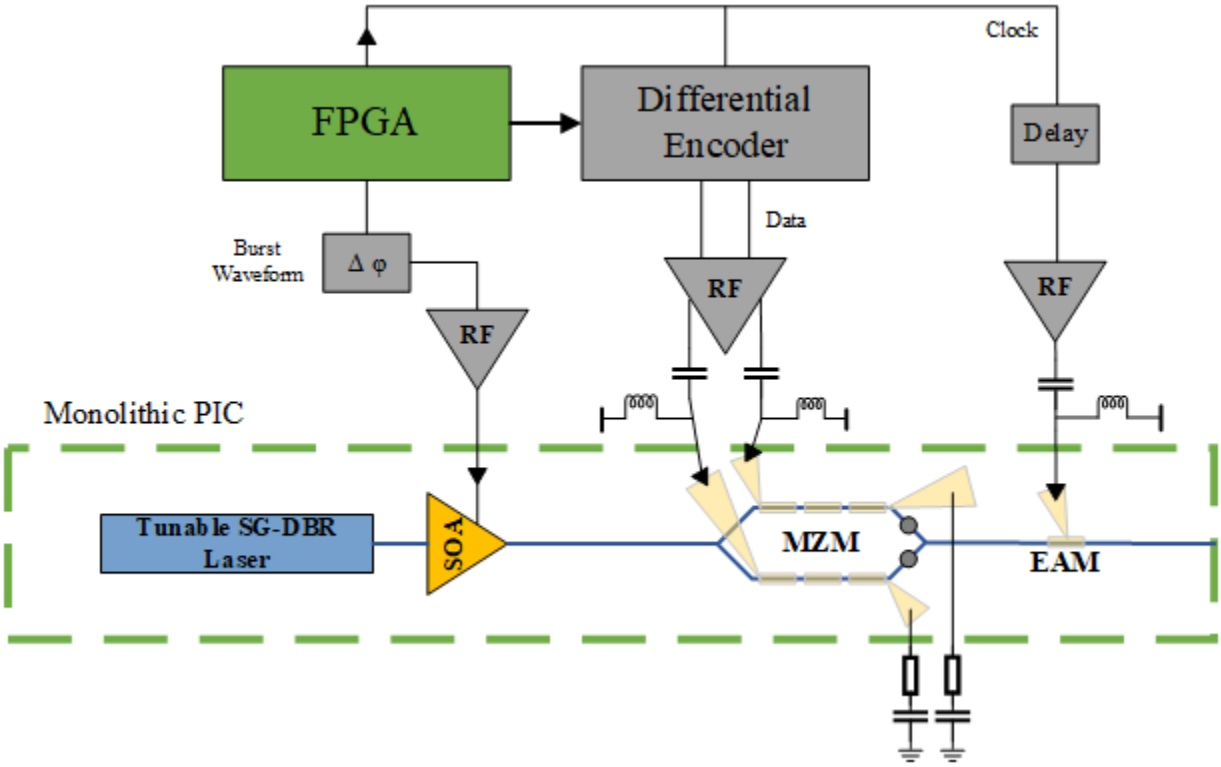

Figure 1. PIC transmitter beside driving electronics. PIC includes an SG-DBR laser, semiconductor optical amplifier (SOA), Mach-Zehnder Modulator (MZM), and electro-absorption modulator (EAM).

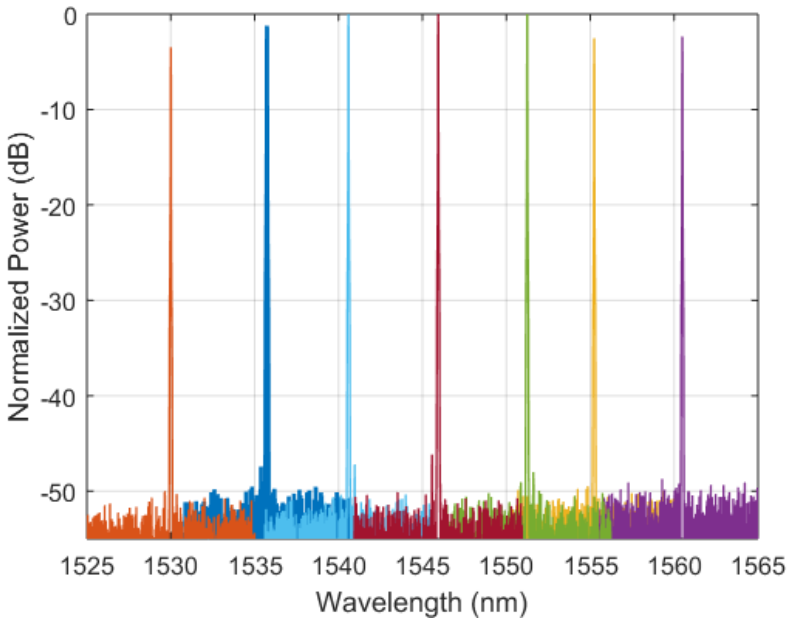

Figure 2. A few overlapped wavelengths of the SG-DBR. Tuning over 30 nm with side mode suppression ratio over 45 dB was obtained.

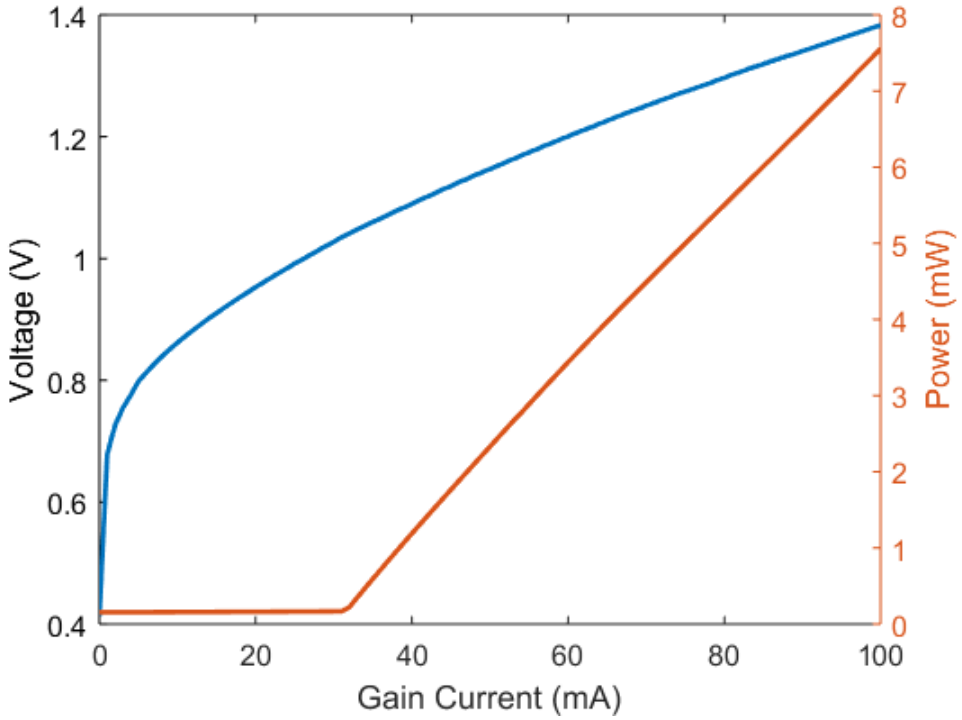

Figure 3. Light-current-voltage curves of integrated SG-DBR showing threshold current of 30 mA and slope efficiency of 0.1 A/W. Output power exceeds 7 mW at 100 mA drive current into the laser gain section.

Following the SG-DBR laser is an SOA for amplification of the laser. The SOA can also be used for multi-rate communication by utilizing burst mode operation and an average power limited amplifier. Such operation boosts the peak power of transmitted symbols over short bursts but maintains the average power. While burst mode operation was not demonstrated here, burst duty cycles as low as 10% would be possible utilizing an SOA with 25 dB extinction as demonstrated in [11] for an SOA over a 4.5V peak-to-peak drive.

A Mach-Zehnder Modulator (MZM) follows the SOA. The MZM is driven differentially with phase shift keying data. For DPSK the MZM is biased at an output null. The interferometer is aligned using current sensitive phase sections. Unlike DPSK, the MZM was aligned at quadrature for NRZ-OOK measurements. While the optimal drive for an MZM generating DPSK is $2V\pi$, an MZM maintains a π phase shift over reduced drives but a penalty in the form of reduced optical signal to noise ratios results. In this work the MZM arms are terminated with DC blocking capacitors in series with thin film resistors of 50 Ω to allow reverse biasing of the MZM and to minimize back reflections respectively.

An electro-absorption modulator (EAM) is then used to carve the 50% RZ pulses at the clock frequency. The EAM is also reverse biased and terminated with a DC blocking capacitor in series with a 50 Ω resistor.

3. TEST SETUP AND DRIVING ELECTRONICS

Figure 4 shows an image of the PIC mounted on custom carrier embedded in an electronics test bed. The PIC is cooled using a thermo electric cooler to a stage temperature of 18 °C. The carrier contains both DC and coplanar waveguide traces. The PCB delivers both amplified high-speed pseudo random binary sequences (PRBS) and biasing to various parts of the PIC using commercial off the shelf (COTS) electronic components. Coarse and fine-tuning circuits on the PCB help tune the MZM phase sections for biasing of the MZM interferometer for various modulation formats. The differential driver also allows variable gain. Integrated bias-T's are also utilized for reverse biasing of the MZM and EAM.

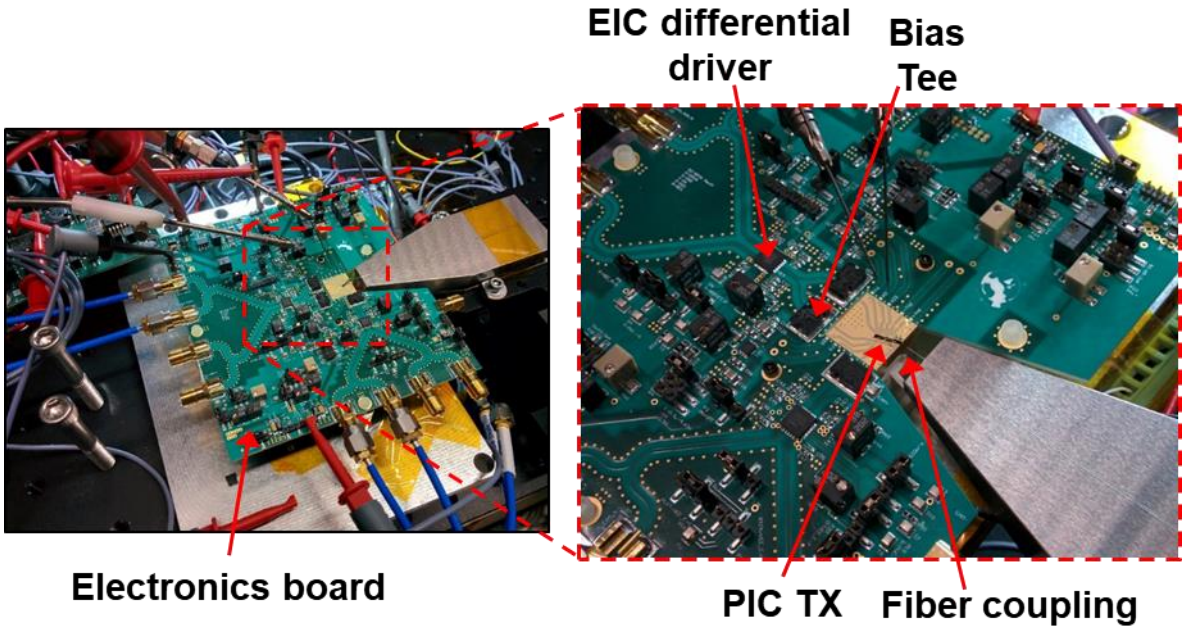

Figure 4. Photograph of electronic test bed with mounted PIC on carrier. Test bed includes biasing and high-speed driving electronics. Light is collected using a lensed fiber.

Figure 5 shows a simplified block diagram of the test setup used to obtain eye diagrams of various modulation formats. Regulated supplies on board a PCB were used for biasing various sections of the PIC. A PRBS was generated off chip and amplified with a commercial driver/amplifier. The PIC was placed at an angle to account for refraction at the facet.

Light was then collected using a lensed fiber, amplified with an erbium doped fiber amplifier (EDFA), and then detected on an optical oscilloscope serving as an intensity module.

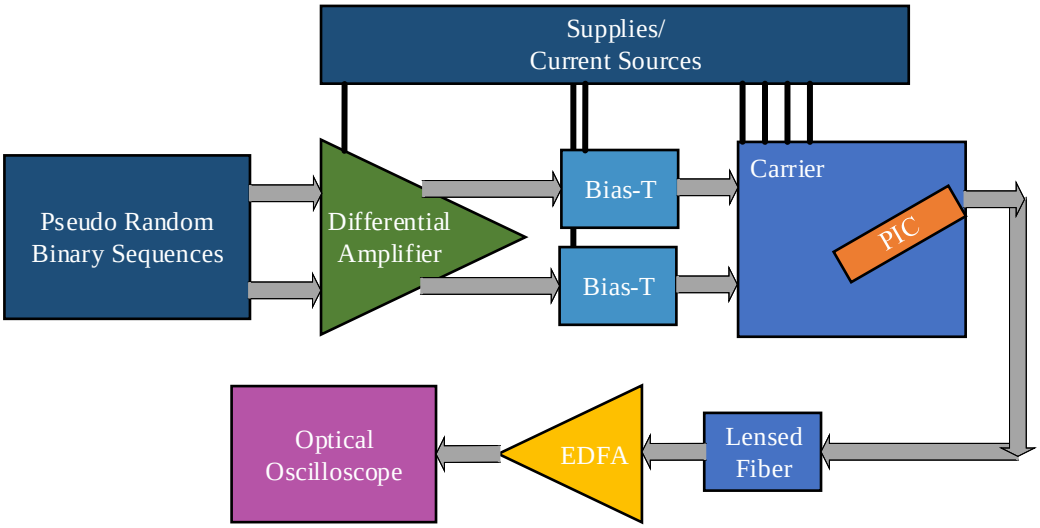

Figure 5. Simplified test setup. Pseudo random binary sequences and clock were amplified on PCB for driving of an MZM and EAM. Coarse and fine-tuning current sources applied biasing to PIC from regulated supplies on PCB.

4. HIGH-SPEED MEASUREMENTS

For high speed measurements, the laser gain section and SOA were biased at 90 mA. Various modulation formats were tested. Figure 6 shows eye diagrams for NRZ-OOK modulation formats at data rates of 2.5, 5, and 10 Gbps. Corresponding extinction ratios were 8.2, 7.8, and 7.6 dB respectively. The NRZ-OOK eye diagrams were obtained by biasing the MZM at quadrature. Each arm of the MZM was reverse biased at -3 V. The MZM was driven at a peak-to-peak differential drive of approximately 4.8V. Filters and better alignment would further improve these results but nevertheless clear eye openings are apparent. Faster rates were not tested due to limitations in the electronic driving hardware. The EAM was not utilized for NRZ-OOK modulation.

Figure 6 also shows 50% RZ-OOK modulation. In this case the EAM was used to carve the RZ pulses. The EAM in this case was reverse biased at -2.5 V and approximately driven with a 2.8 Vpp clock.

Figure 7 shows RZ-DPSK modulation eye diagrams. Here the MZM was biased at a null. Data rates of 2.5 and 5 Gbps are demonstrated. The differential drive was approximately 4.8 Vpp. Unfortunately, optimal electrical driving conditions could not be obtained due to limitations in the electronic test setup and thus limited the extinction ratio to 3-4 dB. Nevertheless, the clear eye diagrams show that the transmitter is suitable for high-speed RZ-DPSK modulation. Further improvements in the electronic setup are required to obtain better extinction ratios.

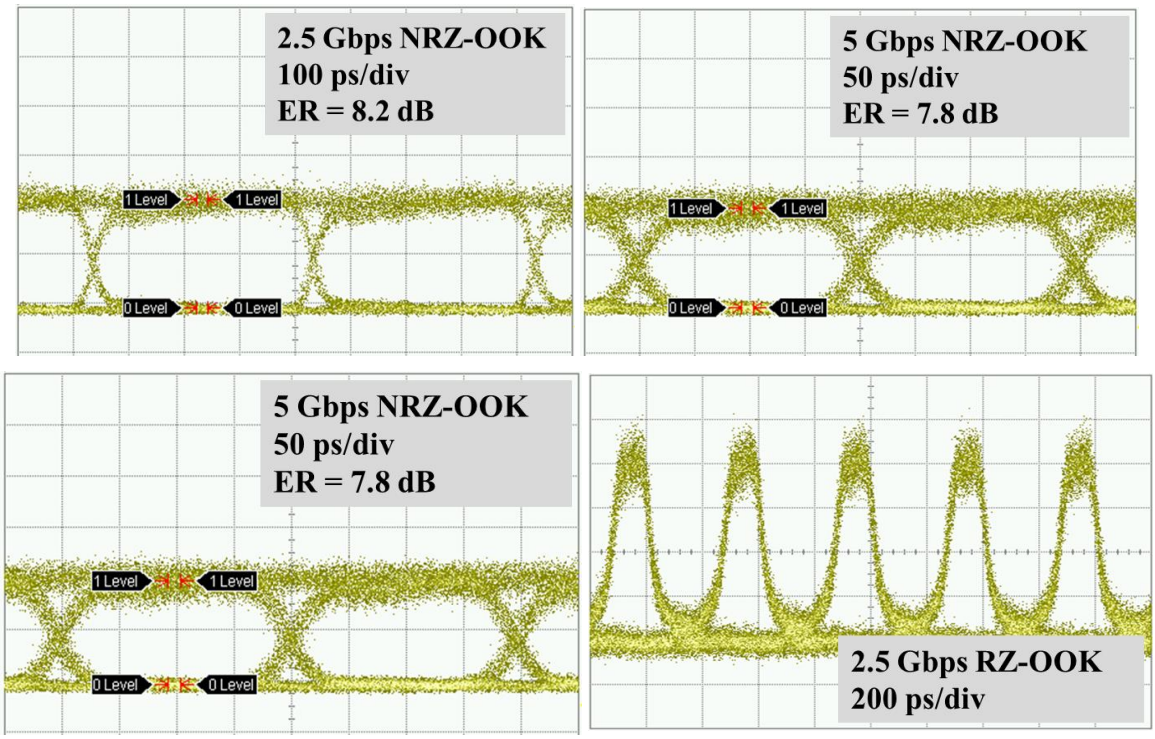

Figure 6. NRZ-OOK eye diagrams at 2.5, 5, 10 Gbps. Clear eye openings at all data rates with extinction ratios of 8.2, 7.8, and 7.6 dB respectively. Also shown 2.5 Gbps RZ-OOK.

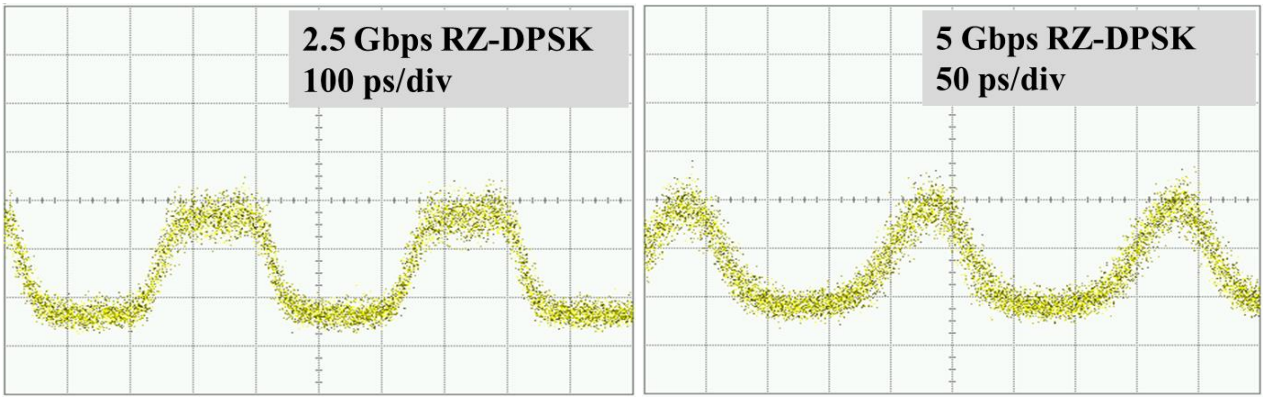

Figure 7. RZ-DPSK eye diagrams at 2.5, and 5 Gbps respectively.

5. SUMMARY

Optical communications will greatly enhance space science and exploration in the near future. Most demonstrations have until thus far utilized communication terminals constructed of discrete optical devices and consequently have high C-SWaP. PICs are of great interest as they allow integration of optical terminals on-chip.

Here we demonstrated a transmitter PIC in an electronics test bed suitable for high data rate RZ-DPSK modulation up to 5 Gbps and DPSK and NRZ-OOK up to 10 Gbps. The PIC includes an SG-DBR laser, SOA, MZM, and EAM. The results are promising for future low C-SWaP space optical communications.

Future work will include RZ-DPSK demodulation with a delay line interferometer, transmission over free-space, and link characterization including bit error rates. Improvements in the electronic hardware are also required for optimal performance of the PIC.

REFERENCES

[1] Don M. Boroson, Bryan S. Robinson, Daniel V. Murphy, Dennis A. Burianek, Farzana Khatri, Joseph M. Kovalik, Zoran Sodnik, Donald M. Cornwell, "Overview and results of the Lunar Laser Communication Demonstration," Proc. SPIE 8971, Free-Space Laser Communication and Atmospheric Propagation XXVI, 89710S (6 March 2014).

[2] Berry Smutny, Hartmut Kaempfner, Gerd Muehlnikel, Uwe Sterr, Bernhard Wandernoth, Frank Heine, Ulrich Hildebrand, Daniel Dallmann, Martin Reinhardt, Axel Freier, Robert Lange, Knut Boehmer, Thomas Feldhaus, Juergen Mueller, Andreas Weichert, Peter Greulich, Stefan Seel, Rolf Meyer, Reinhard Czichy, "5.6 Gbps optical intersatellite communication link," Proc. SPIE 7199, Free-Space Laser Communication Technologies XXI, 719906 (24 February 2009).

[3] D. J. Israel, B. L. Edwards and J. W. Staren, "Laser Communications Relay Demonstration (LCRD) update and the path towards optical relay operations," *2017 IEEE Aerospace Conference*, Big Sky, MT, 2017, pp. 1-6.

[4] B. Isaac, B. Song, S. Pinna, S. Arafin, L. Coldren and J. Klamkin, "Indium Phosphide Photonic Integrated Circuit Transmitter with Integrated Linewidth Narrowing for Laser Communications and Sensing," *2018 IEEE International Semiconductor Laser Conference (ISLC)*, Santa Fe, NM, 2018, pp. 1-2.

[5] Y. Liu *et al*., "Ultra-Low-Loss Silicon Nitride Optical Beamforming Network for Wideband Wireless Applications," in *IEEE Journal of Selected Topics in Quantum Electronics*, vol. 24, no. 4, pp. 1-10, July-Aug. 2018, Art no. 8300410.

[6] V. Rosborough, F. Gambini, J. Snyder, L. Johansson and J. Klamkin, "Integrated transmitter for deep space optical communications," *2016 IEEE Avionics and Vehicle Fiber-Optics and Photonics Conference (AVFOP)*, Long Beach, CA, 2016, pp. 207-208.

[7] H. Zhao *et al*., "Indium Phosphide Photonic Integrated Circuits for Free Space Optical Links," in *IEEE Journal of Selected Topics in Quantum Electronics*, vol. 24, no. 6, pp. 1-6, Nov.-Dec. 2018, Art no. 6101806.

[8] D. O. Caplan *et al*., "Ultra-wide-range multi-rate DPSK laser communications," *CLEO/QELS: 2010 Laser Science to Photonic Applications*, San Jose, CA, 2010, pp. 1-2.

[9] D. O. Caplan, J. J. Carney, J. J. Fitzgerald, I. Gaschits, R. Kaminsky, G. Lund, S. A. Hamilton, R. J. Magliocco, R. J. Murphy, H. G. Rao, N. W. Spellmeyer, J. P. Wang, "Multi-rate DPSK optical transceivers for free-space applications," Proc. SPIE 8971, Free-Space Laser Communication and Atmospheric Propagation XXVI, 89710K (25 March 2014).

[10] W. A. Atia and R. S. Bondurant, "Demonstration of return-to-zero signaling in both OOK and DPSK formats to improve receiver sensitivity in an optically preamplified receiver," *1999 IEEE LEOS Annual Meeting Conference Proceedings. LEOS'99. 12th Annual Meeting. IEEE Lasers and Electro-Optics Society 1999 Annual Meeting (Cat. No.99CH37009)*, San Francisco, CA, USA, 1999, pp. 226-227 vol.1.

[11] Joseph Fridlander, Sergio Pinna, Victoria Rosborough, Steven Estrella, Leif Johansson, Jonathan Klamkin, "RZ-DPSK photonic integrated transmitter for space optical communications," Proc. SPIE 10524, Free-Space Laser Communication and Atmospheric Propagation XXX, 105240Y (15 February 2018).